Instantaneous Baseline Damage Localization Using Sensor Mapping

Mohammad Saleh Salmanpour, *Student Member, IEEE*, Zahra Sharif Khodaei, and Mohammad Hossein Aliabadi

***Abstract*— In this paper, an instantaneously recorded baseline method is proposed using piezoelectric transducers for damage localization under varying temperature. This method eliminates need for baselines required when operating at different temperatures by mapping a baseline area onto the interrogation area. Instantaneously recorded baselines and current interrogation signals are calibrated based on the sensor mapping. This allows the extraction of damage scatter signal which is used to localize damage. The proposed method is used to localize actual impact damage on a composite plate under varying temperatures. The method is also applied to a stiffened fuselage panel to accurately localize impact damage.**

***Index Terms*— Ultrasonic, lamb waves, piezoelectric, non-destructive testing, structural health monitoring, impact damage, composites, BVID.**

I. Introduction

THE susceptibility of composite materials to impact damage has forced a damage tolerant design approach in aircraft, driven by certification requirements [1]. An area of great concern is barely visible impact damage (BVID) which can lead to a drop in strength properties of Carbon fibre reinforced polymers (CFRPs). Structural health monitoring (SHM) systems can allow real-time, in-situ integrity assessments with minimal intrusion to the normal operation schedule. This will lead to savings through lighter composites and a more efficient condition based maintenance philosophy. Ultrasonic Guided wave active SHM systems are composed of a network of attached ultrasonic transducers, typically piezoelectric Lead Zirconate Titanate (PZT), to generate and sense diagnostics Lamb waves. These are sensitive to the material and geometric properties of the host structure, and presence of damage [2]–[5].

In baseline comparison methods the current and baseline signals are subtracted, the envelope of this is referred to as the residual signal. The presence of damage would cause scattering and mode conversion, the residual must only contain damage scattered signal or mode conversions for accurate damage position localization. The focus of this work is on CFRP material and localization of BVID which could include delamination. The underlying elegance of baseline comparison is that the highly convoluted Lamb wave response of the geometric features are removed leaving only the damage scattered signal [2], [3]. This allows damage detection and localization on complex and anisotropic structures, with manufacturing tolerances.

Environmental conditions can significantly alter Lamb wave propagation. Changes in conditions between the baselines will cause non-damage related residual, significantly reducing the accuracy of damage detection and localization [6]–[8]. Temperature in particular can significantly influence Lamb wave propagation. Aircraft may be exposed to a wide range of temperatures during normal operation. Damage detection may need to be performed at a range of temperatures without access to climate controlled hangers. The effects of temperature are many-fold with changes in the waveguide material properties, size dilation and changes in transducer material properties. The most dominant effect being temperature dependence of the waveguide (host structure) elastic moduli [9]. Relative humidity levels also have an impact on propagation in CFRPs; due to moisture absorption, but on a longer time scale than temperature [10].

Not relying on previously recorded baselines is a possible solution to changing environmental conditions. [11] proposed a reference free method exploiting dual transducer arrangements to selectively actuate and sense Lamb wave modes. Transducer paths effected by damage were found by excitation of a particular wave mode. Wave mode propagation and arrival times must be characterised beforehand. Other reference free approaches exploit the non-linear nature of damage scatter, arguing these are not time reversible [12] or scalable [13]. Hybrid methods have been developed [14]–[16] proposed an enhanced sensitivity time reversal method. However the time reversal process also removes time of arrival information, vital for high spatial accuracy damage localization [14]. Scaled subtraction was applied to a composite panels to detect delaminations [17]. These methods may not perform well on real structures with complex features, such as changes in thickness; stiffeners and bolts, can also cause non-linear wave propagation.

The method proposed uses instantaneous baselines for damage localization based on sensor mapping and incorporates a delay and sum algorithm. The problem of environmental conditions and temperature change is mitigated as baselines are recorded at the same time as the current signal. This means temperature compensation is not required while accurate detection is achieved over a larger temperature range than [8]. The novelty is in using calibrated instantaneous baselines by

Manuscript received September 26, 2016; accepted November 10, 2016. Date of publication November 18, 2016; date of current version December 20, 2016. This work was supported in part by the Engineering and Physical Sciences Research Council Doctoral Training Account and in part by the European Union's Seventh Framework Program for Research, Technological Development, and Demonstration under Grant 284562. The associate editor coordinating the review of this paper and approving it for publication was Dr. Stefan J. Rupitsch.

The authors are with the Department of Aeronautics, Imperial College London, London, SW72AZ, U.K. (e-mail: mohammad.salmanpour@imperial.ac.uk; z.sharif-khodaei@imperial.ac.uk; m.h.aliabadi@imperial.ac.uk).

Digital Object Identifier 10.1109/JSEN.2016.2629279

mapping transducers from a baseline area to localize damage within an interrogation area. Sensor calibration removes the non-damage related residual that is present even in the pristine state when mapping a baseline area onto an interrogation area. It is shown that the calibrated residual allows extraction of the damage scatter signal, allowing accurate localization using time of arrival and amplitude. Sensor placement optimisation has been shown to be an important factor in damage localization accuracy [18], [19], with the optimal arrangements typically symmetric or evenly spaced transducers around structural features. [20] also used evenly spaces transducer or sub areas in multilevel baseline comparison approach. The proposed method exploits symmetry (or partial symmetry) of the structure even in complex structures such as curved stiffened composite panels. The method is demonstrated experimentally by localizing actual impact induced BVID in a CFRP plate and BVID under a stiffener foot in a CFRP fuselage panel.

II. Instantaneous Baseline Method

The proposed instantaneous baseline method generates calibrated baselines recorded at the same time as the current/damaged signal. That is, for a given interrogation path a geometrically similar path is used as an instantaneous baseline under the same conditions. The signal is calibrated allowing it to be used as an input for standard baseline comparison approaches to localize damage. In this paper the delay and sum algorithm is used. The delay and sum algorithm is not the focus of this paper and the reader is referred to exhaustive works such as [2], [3], and [21]. In this method the structure is discretised into points. Using the propagation velocity, the time of flight (TOF) for the path actuator-point-sensor is calculated for each point. The residual value for a given actuator-sensor path is found at the TOF corresponding to each point. If damage is located at that point the residual value will be higher than others. The recorded residual values at each point are then fused for all transducer paths to form a damage probability map. This then highlights the most probable location of damage.

Detections methods relying on previously recorded baseline sets have an integral link to the structure with an inbuilt ability to deal with complex geometries. These can directly isolate damage scatter waves in the time domain:

$$\begin{aligned} B_i &= G + \Delta_i, \quad C_i = G + D_i + \Delta_i \\ R_{ii} &= env(C_i - B_i) \\ &= env(D_i) \end{aligned} \tag{1}$$

Both baseline B_i and the current signal C_i will contain the wave propagation profile G due to the geometry. Crucially they will both contain wave features due to the geometric uncertainties and manufacturing tolerances Δ_i, unique to the particular path i. Subtracting baseline and current signals will remove G as well as Δ_i particular to that path, leaving only the damage scatter signal D_i in the residual envelope R_{ii}.

By mapping a baseline area onto a geometrically similar inspection area it is possible to use instantaneous baselines as shown in Figure 1. However the inherent ability to deal with complex manufacturing tolerances and geometric uncertainties

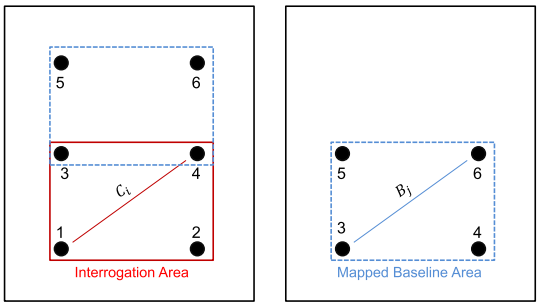

Fig. 1. Geometrically similar baseline area mapped onto inspection area allowing instantaneous baselines.

is lost, as is the case with most baseline free approaches. This is because if the baseline path j is mapped on to the current interrogation path i, the residual envelope R_{ij} is not comprised only of the damage features. It also contains features Δ_i and Δ_j unique to the paths i and j:

$$\begin{aligned} B_j &= G + \Delta_j, \quad C_i = G + D_i + \Delta_i \\ R_{ij} &= env(C_i - B_j) \\ &= env(D_i + \Delta_i - \Delta_j) \end{aligned} \tag{2}$$

To minimises the mismatch associated with transducer path mappings, the proposed method applies a calibration for each specific path mapping. The calibration revolves around finding the pristine difference envelope between each transducer path:

$$\begin{aligned} L_{ij} &= env(B_i - B_j) \\ &= env(\Delta_i - \Delta_j) \end{aligned} \tag{3}$$

The mapping calibration L_{ij} is then used to remove the non-damage related features, to yield a calibrated residual envelope R^c_{ij} which contains only the damage scatter signal envelope:

$$\begin{aligned} R^c_{ij} &= R_{ij} - L_{ij} \\ &\approx env(D_i) \end{aligned} \tag{4}$$

The sparse transducer array must be arranged to form repeating cells, and each cell can act as the baseline for other cells. Transducers should be arranged in a way to achieve local symmetry, even if the structure is not globally symmetric. For example they should be positioned symmetrical around a stiffener. Anisotropic material can be interrogated (e.g. CFRP with uni-direction fibre layup) but this will reduced the number of possible cell mappings, as the fibre direction must be preserved.

It is possible to localize damage without prior knowledge of the location. To select the interrogation area and the baseline area, it is possible to identify a cell with large levels of residual with respect to the other cells. This assumes damage is confined to one cell. If a damaged cell is used as the baseline area, damage will be predicted in every cell at the corresponding location, this is readily detectable as false alarm. In addition overlapping cell mappings would allow a unique damage point to be identified.

III. Experimental Set-Up

Experiments were conducted to demonstrate the developed instantaneous baseline method. The data acquisition process,

experimental set-up and properties of the CFRP composite plate and fuselage panel are described in this section.

Ultrasonic signals were recorded using a National Instruments platform. This consisted of a PXIe 5412 single channel arbitrary voltage generator, PXIe 5105 digital oscilloscope card and a Pickering 40-726A switching card with maximum output voltage amplitude of 12 volts. Piezoeletric (PZT) transducers are used to actuate and sense Lamb waves. Lamb waves were excited with a five cycle Hanning tone-burst with central frequency swept in the range of 50-350 kHz. This ensured signals were available at both low (50 kHz) and high (300 kHz) frequencies with dominant A_0 and S_0 modes respectively. The response was sampled at 60 MS/s for 0.001 seconds. Each recording was repeated 10 times, bandpass filtered and averaged. Transducers were permanently mounted on one side of the structure. The plate was heated in a TAS ECO 135 environmental chamber. To induced BVID an Instron CEAST 9350 drop tower with a hemispherical impactor of diameter 20 mm was used.

A. Composite Plate

The CFRP composite plate consisted of 16 unidirectional Hexply 914-TS-5-134 plies with stacking sequence $[0,45,-45,90]_{2s}$, with 2 mm overall thickness. 9 DuraAct transducers were attached to the top side of the plate using Hexcel Redux 312 film adhesive depicted in Figure 2. Signals at a range of frequencies were recorded, at −17, 0, 22, 40 and 60°C. The highest temperature was chosen such to cover the highest air temperatures as specified by MIL-STD 180G [22]. Uniform temperature profile was achieved by holding temperature constant for 30 minutes. Results presented are for 50 kHz as it was found the dominant A_0 mode at this frequency showed good sensitivity to the presence of damage.

The plate was subjected to a 4.82 J impact (mass 2.41 kg) with the drop tower. This was the lowest impactor mass and energy found to cause damage with this set-up, in an effort to induce the lowest severity damage (BVID) possible. The BVID was undetectable by eye, with no visible marking on the either side. Presence of the BVID was confirmed with a Dolphi-cam scanner producing a C-Scan image shown in Figure 2a.

B. Fuselage Panel

The fuselage panel used in this section had overall measurements 790 × 1150 mm and 1978 mm radius of curvature to the outer surface. 16 DuraAct transducers, were bonded to the surface with cyanoacrylate Loctite 401 adhesive. These were equally spaced about the stiffeners as shown in Figure 3. Transducers were mounted on the concave side as this was the inner part of the fuselage.

The panel skin and omega hat stiffeners were made using T800/M21 unidirectional pre-pregs and manufactured to Airbus standards [23]. The skin and stiffeners had thickness/layup 1.656 mm [45/−45/90/0/90/0/90/−45/45] and 1.288 mm [45/−45/0/90/0/−45/45] respectively.

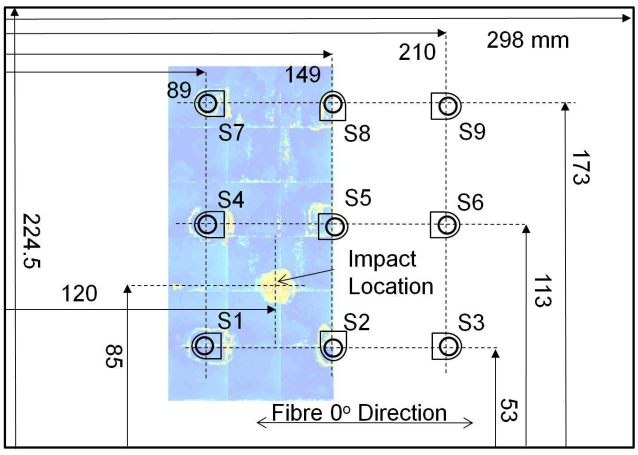

(a)

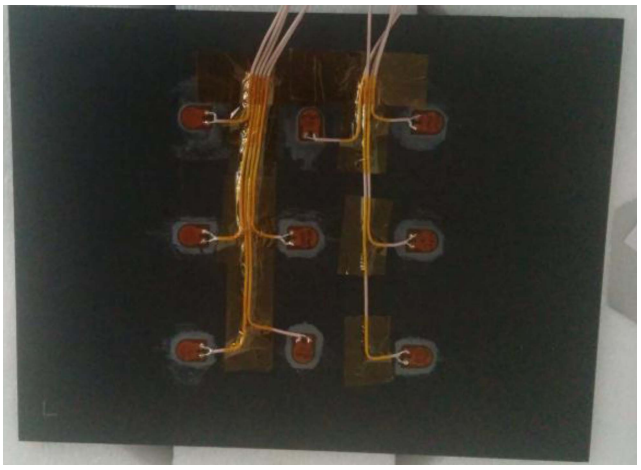

(b)

Fig. 2. CFRP composite plate with 9 DuraAct transducers. (a) C-Scan overlaid on plate schematic. (b) Actual plate used.

The panel was subjected to a single 40 J impact on the convex/outer surface, inducing BVID. Both finite element simulations and experimental results showed after *two* such impacts there was a 10% reduction in compressive strength compared to the pristine cases of 340 and 336 kN [24]. After the first impact C-Scan results confirmed the presence of damage which was undetectable with the naked eye.

The interrogation area was situated at the centre of the panel, while the two available baseline areas where on either side. The areas were geometrically similar in that the area covered contained the same geometric features and spacing: stiffener and skin. However, the areas were not identical: distances to panel boundaries, bolts and attachment points were different between the interrogation and the mapped baseline transducers.

IV. Damage Feature Extract

The main challenge of the proposed method is removal of non-damage related residual while preserving damage features. This can be demonstrated by comparing a path with damage in the direct path and another far from the direct path, shown as path 1 and path 3 respectively in Figure 4.

For damage located far from the direct path, the actual damage residual R_{33} is very low, and only apparent after

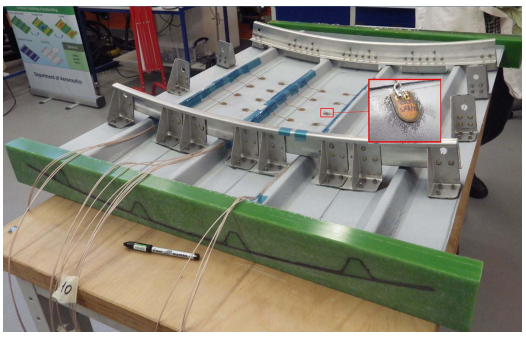

(a)

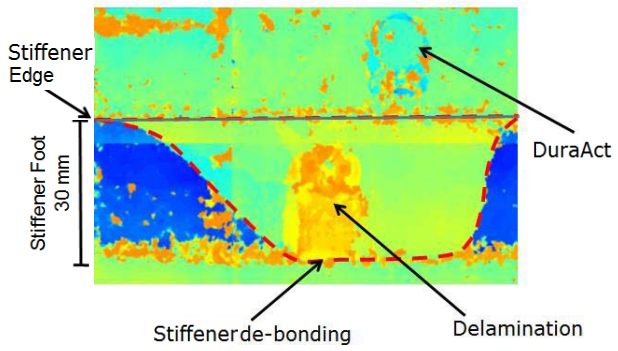

(b)

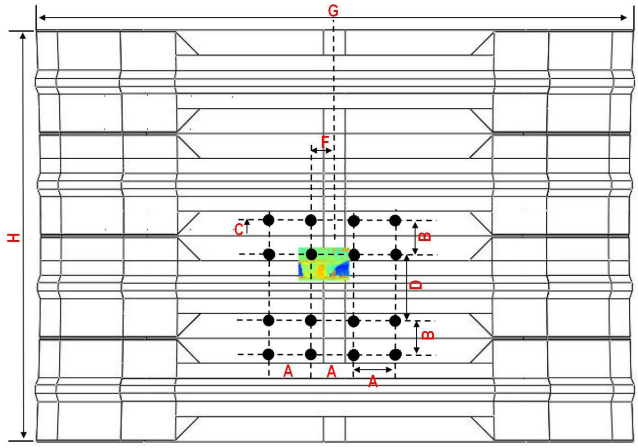

(c)

Fig. 3. CFRP Fuselage panel schematic and C-Scan after impact. C-Scan and schematic courtesy [24]. (a) Panel during data acquisition. (b) C-Scan from impacted side. (c) Black circles are DuraAct transducers. A=70, B=65, D=133, C=32.5, F=35, G=1150, H=790 mm.

the first wave packet. Calibrated residual R_{34} has a large peak at the first wave packet. This is inconsistent with the actual damage residual and is clearly not due to damage but manufacturing tolerances. By applying the pre-recorded calibration envelope this can be removed, yielding calibrated residual R^c_{34} very close to zero as shown in Figure 5b.

With damage in the direct path, the actual damage residual R_{11} has a large peak at the same time as the first wave packet, as shown in Figure 5a. It can be observed that the un-calibrated R_{12} has a higher first peak than the actual damage residual R_{11}. Applying the calibration yields a R^c_{12} that has an almost identical first peak as R_{11} with the arrival time preserved. Hence the damage features are preserved while non-damage wave features are removed.

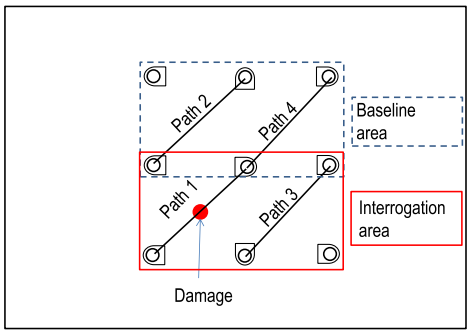

Fig. 4. CFRP plate with impact damage. Path 2 acts as instantaneous baseline for paths 1, and 4 for 3.

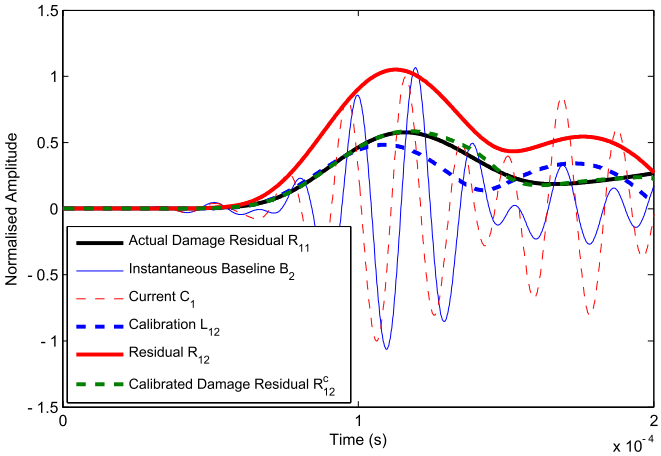

(a)

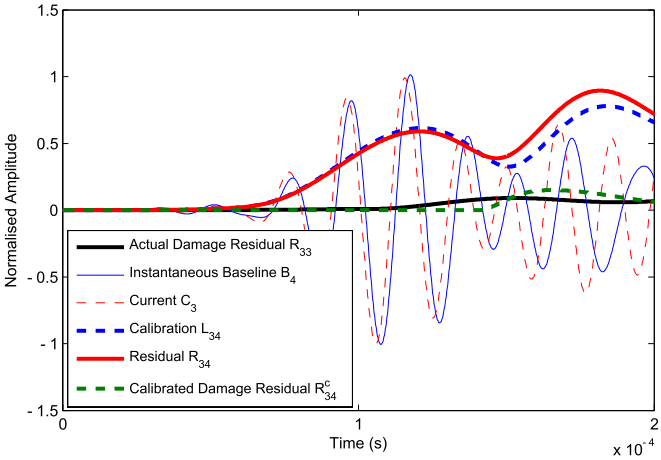

(b)

Fig. 5. Signals from impacted CFRP composite plate (2×50 mm.kHz). (a) Path containing BVID. (b) Path far from BVID.

Predictably the calibration envelope will show a shift corresponding to the temperature dependence of the wave propagation velocity. Crucially as all phase information is discarded in the calibration envelope, there is only a minor change in the calibrated residual compared to the case when there is no temperature difference, or even the actual residual, as shown in 6a. In comparison, normal signal subtraction leaves a non-damage related residual that could mask the presence of damage as shown in Figure 6b and is larger than the damage residual shown in Figure 5a.

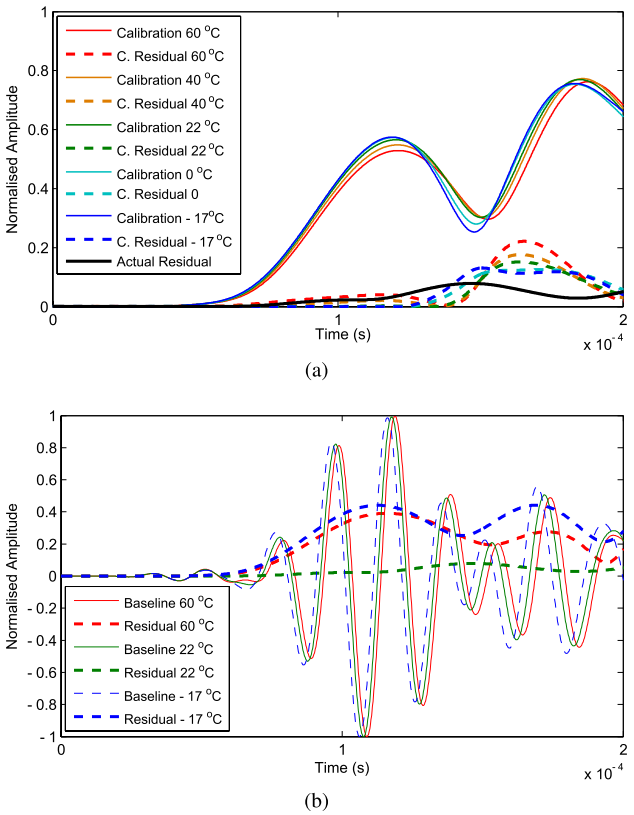

Fig. 6. Signals for an impacted CFRP composite plate (2×50 mm.kHz) at various temperatures, current signal C_3 at 22 °C. (a) Calibration envelopes L_{34} and calibrated residuals R^c_{34} at different tempereatures. (b) Normal signal subtraction R_{33}, with B_3 at different temperatures.

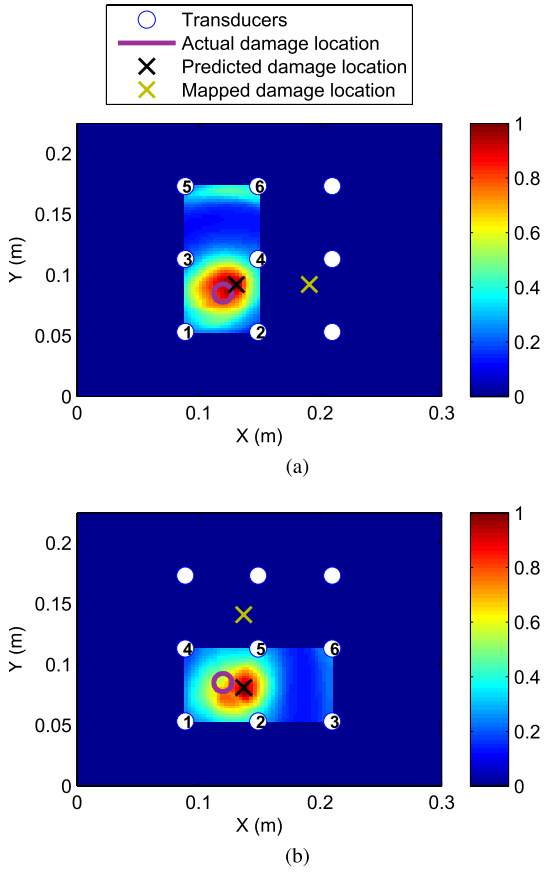

Fig. 7. Instantaneous baseline damage probability map of a CFRP plate with BVID, calibration temperature difference 38 °C (2×50 mm.kHz). (a) Mapping 1 and (b) mapping 2.

It must be noted that the temperature can be unknown. Temperature values at the time of recording have been explicitly mentioned here only to demonstrate robustness of the approach.

V. Results and Discussion

Experimental results for detection of damage on two structures are presented. Both the CFRP flat plate and fuselage panel have been impacted leading to BVID.

The damage probability maps shown in Figures 7 and 8a numbered markers indicate the interrogation area transducers while the blank markers indicate the instantaneous baseline mapped transducers.

A. Composite Plate

Using the instantaneous baseline method proposed it possible to locate the impact damage as apparent in Figure 8.

The instantaneous baseline was applied to signal recorded at 22 °C. The calibration envelopes were recorded at a temperature range between −17 to 60 °C, a temperature difference of −39 and +38 °C respectively. Results for calibration recorded at a temperature difference of 38 °C are presented in Figure 7. A normal delay and sum method will fail at this level of temperature variation. It was found that in all cases damage was localized to within 17.6 mm of the impact location (or 10.1 mm from the edge of the damage), see table I. The error due to mapping alone (no temperature difference) was greater than the additional error due to temperature difference.

TABLE I

Localization Error of BVID on CFRP Plate, Actual Location (120,85) mm. Calibration Recorded at Range of Temperatures, Instantaneous Baseline Recorded at 22 °C

Calibration Temperature (°C)	Mapping	Localization (mm)		Absolute Error (mm)
		x	y	
-17	1	131.1	92.1	13.1
-17	2	131.1	78.6	12.8
0	1	131.1	89.8	12.1
0	2	131.1	76.3	14.1
25	1	128.1	87.6	8.5
25	2	125.2	74.1	12.1
40	1	128.1	89.8	9.4
40	2	122.2	74.1	11.1
60	1	131.1	89.8	12.1
60	2	137.1	80.8	17.6

It was found that the vertical mapping (mapping 1) was more accurate with mean error of 11 mm while the horizontal mapping (mapping 2) had mean error of 13.5 for all temperature differences. This can be associated to mappings used. The mappings preserved fibre directions. However, in both mappings the baseline and interrogation areas were not equally spaced about the boundaries. Mapping 1 preserved both the baseline and interrogation area distances to the top and bottom boundaries, while mapping 2 preserved the distances to the left

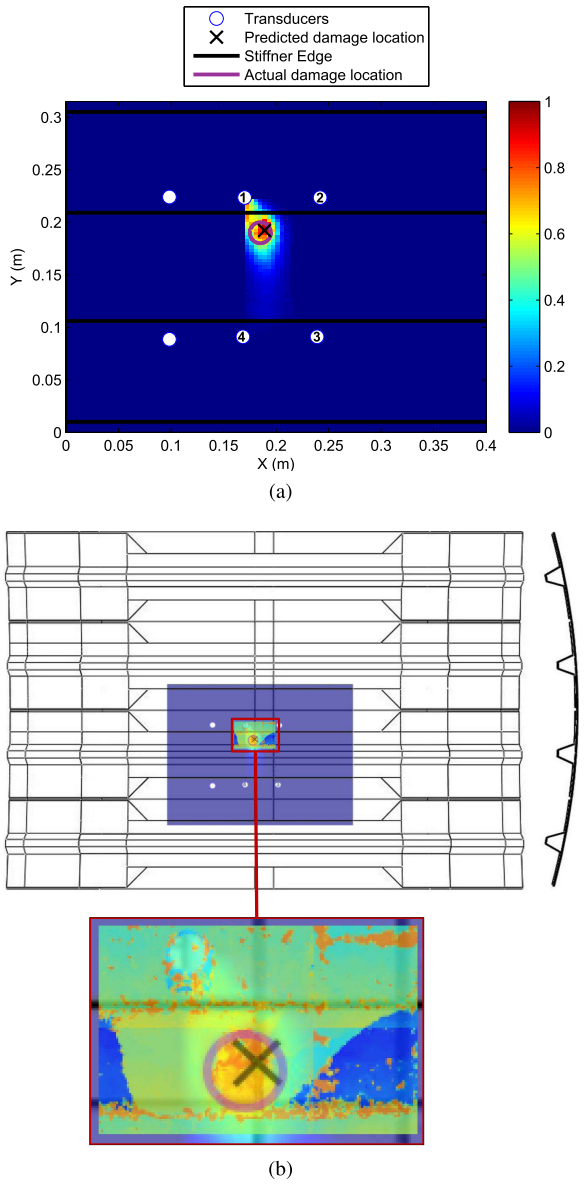

Fig. 8. Instantaneous baseline method applied to a stiffened composite fuselage panel. (a) Damage probability map. (b) Damage probability map with the panel schematic overlaid on the C-Scan. C-Scan and CAD drawing courtesy [24].

and right boundaries. The distances to the top/bottom boundaries were shorter than the left/right boundaries. Hence when not preserved the top/bottom boundaries have a larger impact on the accuracy due to boundary reflections arriving earlier and interfering with the damage scattered waves, as observed in mapping 2.

B. Fuselage Panel

The fuselage panel BVID was localized accurately, as shown in 8a. This was in an area of non-uniform thickness and the interrogation area being non-symmetric with respect to the panel boundaries.

The interrogation area was situated at the centre of the panel, while the two available baseline areas where on either side. The areas were geometrically similar in that the area covered contained the same geometric features and spacing, e.g. stiffener and skin. However, the baseline areas were not geometrical identical to the interrogation area. That is the distances to the panel boundaries were different between the interrogation and the mapped baseline transducers. The damage prediction was within the area of the delamination.

VI. Conclusions

This paper presented a baseline free method for localizing damage using guided wave ultrasonic signals. Baseline comparison methods, including delay and sum are not able to detect or localize damage without access to a large data set of pristine results recorded at a range of operating temperatures. Signal temperature compensation is also limited in the applicable temperature range. The developed method uses instantaneous baseline signals recorded at the same time as the current interrogation signal hence overcoming the problem of temperature change. The underlying strength is accurate localization in complex structures (CFRP, curved, stiffened and with attachment points and bolt holes).

The developed method involved mapping of signals from a baseline area onto an interrogation area/cell, with all signals recorded at the same time. By calibrating the signals based on the mapping used, it was possible to extract damage scatter signals, free from the influence of manufacturing and geometrical tolerances. It was shown that damage could be localized without prior knowledge of its location.

The method was demonstrated for detection and localization of BVID on a CFRP composite plate. It was shown that the developed method is robust to temperature change, accurately localizing damage. The method was also successfully applied for detection of a crack representative of fatigue on an aluminium plate with 12 transducers (not presented here). An actual stiffened composite fuselage panel was subjected to an impact causing BVID under the stiffener foot. The predicted location of damage on the fuselage panel agreed well with the C-Scan results.

The mapping method requires transducers to be arranged evenly around structural features. Though not an inherent flaw and is typically the case, this may limit flexibility in arrangement. The main weakness of the method is the assumption that damage is confined to one transducer area/cell, additionally any environmental effects must be global and impact all cell equally. Future work will address detection of multiple damages and also the robustness to other environmental conditions (such as vibration) will be examined.

References

[1] EASA, "Acceptable means of compliance (amc) 20-29," *General Acceptable Means of Compliance for Arworthiness of Products, Parts and Appliances. Composite Aircraft Structure*, 2010.

[2] Z. Sharif-Khodaei and M. H. Aliabadi, "Assessment of delay-and-sum algorithms for damage detection in aluminium and composite plates," *Smart Mater. Struct.*, vol. 23, no. 7, p. 075007, 2014.

[3] J. E. Michaels, "Detection, localization and characterization of damage in plates with an *in situ* array of spatially distributed ultrasonic sensors," *Smart Mater. Struct.*, vol. 17, no. 3, p. 035035, 2008.

[4] D. Gao, Y. Wang, Z. Wu, G. Rahim, and S. Bai, "Design of a sensor network for structural health monitoring of a full-scale composite horizontal tail," *Smart Mater. Struct.*, vol. 23, no. 5, p. 055011, 2014.

[5] L. Si and H. Baier, "Real-time impact visualization inspection of aerospace composite structures with distributed sensors," *Sensors*, vol. 15, no. 7, pp. 16536–16556, 2015.

[6] Y. Lu and J. E. Michaels, "Feature extraction and sensor fusion for ultrasonic structural health monitoring under changing environmental conditions," *IEEE Sensors J.*, vol. 9, no. 11, pp. 1462–1471, Nov. 2009.
[7] O. Putkis, R. P. Dalton, and A. J. Croxford, "The influence of temperature variations on ultrasonic guided waves in anisotropic CFRP plates," *Ultrasonics*, vol. 60, pp. 109–116, Jul. 2015.
[8] M. S. Salmanpour, Z. S. Khodaei, and M. H. Aliabadi, "Guided wave temperature correction methods in structural health monitoring," *J. Intell. Mater. Syst. Struct.*, Jun. 2016, doi: 10.1177/1045389X16651155.
[9] G. Konstantinidis, B. W. Drinkwater, and P. D. Wilcox, "The temperature stability of guided wave structural health monitoring systems," *Smart Mater. Struct.*, vol. 15, no. 4, pp. 967–976, 2006.
[10] K. J. Schubert and A. S. Herrmann, "On the influence of moisture absorption on Lamb wave propagation and measurements in viscoelastic cfrp using surface applied piezoelectric sensors," *Compos. Struct.*, vol. 94, no. 12, pp. 3635–3643, 2012.
[11] Y.-K. An, H. J. Lim, M. K. Kim, J. Y. Yang, H. Sohn, and C. G. Lee, "Application of local reference-free damage detection techniques to in situ bridges," *J. Struct. Eng.*, vol. 140, no. 3, p. 04013069, 2014.
[12] H. W. Park, H. Sohn, K. H. Law, and C. R. Farrar, "Time reversal active sensing for health monitoring of a composite plate," *J. Sound Vibrat.*, vol. 302, nos. 1–2, pp. 50–66, 2007.
[13] M. Scalerandi, A. S. Gliozzi, C. L. E. Bruno, and K. Van Den Abeele, "Nonlinear acoustic time reversal imaging using the scaling subtraction method," *J. Phys. D, Appl. Phys.*, vol. 41, no. 21, p. 215404, 2008.
[14] J. Cai, L. Shi, S. Yuan, and Z. Shao, "High spatial resolution imaging for structural health monitoring based on virtual time reversal," *Smart Mater. Struct.*, vol. 20, no. 5, p. 055018, 2011.
[15] W. Wu, W. Qu, L. Xiao, and D. J. Inman, "Detection and localization of fatigue crack with nonlinear instantaneous baseline," *J. Intell. Mater. Syst. Struct.*, vol. 27 no. 12, pp. 1577–1583, Jul. 2016, doi: 10.1177/1045389X15596851.
[16] J. K. Agrahari and S. Kapuria, "A refined Lamb wave time-reversal method with enhanced sensitivity for damage detection in isotropic plates," *J. Intell. Mater. Syst. Struct.*, vol. 27, no. 10, pp. 1283–1305, 2015.
[17] J. Hettler, M. Tabatabateipour, S. Delrue, and K. Van Den Abeele, "Application of the probabilistic algorithm for ultrasonic guided wave tomography of carbon composites," in *Proc. Int. Congr. Ultrason. (ICU)*, May 10–14, 2015, Metz, France.
[18] M. S. Salmanpour, Z. S. Khodaei, and M. H. Aliabadi, "Transducer placement optimisation scheme for a delay and sum damage detection algorithm," *Structural Control Health Monitor.*, 2016.
[19] M. Thiene, Z. S. Khodaei, and M. H. Aliabadi, "Optimal sensor placement for maximum area coverage (mac) for damage localization in composite structures," *Smart Mater. Struct.*, vol. 25, no. 9, p. 095037, 2016.
[20] L. Qiu, X. Qing, and S. Yuan, "A quantitative multi-damage monitoring method for large-scale complex composite," *Struct. Health Monitor.*, vol. 12, no. 3, pp. 183–196, 2013.
[21] Z. Su and L. Ye, *Identificat. Damage Using Lamb Waves: From Fundamentals to Applications*, vol. 48. Springer, 2009.
[22] *Environmental Engineering Considerations and Laboratory Tests*, document MIL-STD-180G, Department Of Defense Test Method Standard, 2008.
[23] M. van Wijngaarden, "Flat and curved panel manufacturing," in *Smart Intelligent Aircraft Structures (SARISTU)*, P. C. Wölcken and M. Papadopoulos, Eds. Switzerland: Springer, 2016, pp. 645–666.
[24] S. Psarras *et al.*, "Compression after multiple impacts: Modelling and experimental validation on composite curved stiffened panels," in *Smart Intelligent Aircraft Structures (SARISTU)*, P. C. Wölcken and M. Papadopoulos, Eds. Switzerland: Springer, 2016, pp. 681–689.

Mohammad Saleh Salmanpour (S'16) received the M.Eng. (Hons.) degree in aeronautical engineering from the Department of Aeronautics, Imperial College London, in 2013, where he is currently pursuing the Ph.D. degree.

Zahra Sharif Khodaei received the Ph.D. degree in numerical modeling of functionally graded materials from Czech Technical University at Prague, Prague, in 2008. She is currently a Lecturer in aerostructures with the Department of Aeronautics, Imperial College London.

She was a Research Associate with the Department of Aeronautics, Imperial College London from 2009 to 2014. She has focused her research on fatigue modeling and analysis of metallic and fiber metallic laminates, more significantly in development of technologies, and methodologies for structural health monitoring of composite structures.

Mohammad Hossein Aliabadi was a Reader and the Head of the Damage Tolerance Division, WIT, Southampton, from 1987 to 1997. He was a Professor of Computational Mechanics and the Director of Aerospace Engineering with Queen Mary, University of London, from 1997 to 2004. He is currently the Head of the Department of Aeronautics, Imperial College London.

His research interests are in the areas of computational structural mechanics, structural health monitoring, fracture mechanics and fatigue, multiscale modeling, and boundary, meshless, and finite-element methods. He has over 500 papers in the above areas, which include over 250 journal publications and 50 authored or edited books. He has supervised close to 50 Ph.D. students.

He is currently a Professor of Aerostructures and Zaharoff Professor of Aviation. He is a Fellow of the Royal Aeronautical Society and the Institute of Mathematics and its Applications.